


RESEARCH

Open Access



Application of 3D bioprinting technology apply to assessing Dangguinantongtang (DGNT) decoctions in arthritis

Zhichao Liang^{1,2,3,4†}, Yunxi Han^{1,3,4†} , Tao Chen^{1,3,4,7†}, Jinwu Wang^{6,7}, Kaili Lin⁸, Luying Yuan^{1,3,4}, Xuefei Li^{1,3,4}, Hao Xu^{1,3,4}, Tengteng Wang^{1,3,4}, Yang Liu^{1,3,4*}, Lianbo Xiao^{2,5*} and Qianqian Liang^{1,3,4*}

Abstract

The aim of this study was to develop a three-dimensional (3D) cell model in order to evaluate the effectiveness of a traditional Chinese medicine decoction in the treatment of arthritis. Chondrocytes (ATDC5) and osteoblasts (MC3T3-E1) were 3D printed separately using methacryloyl gelatin (GelMA) hydrogel bioinks to mimic the natural 3D cell environment. Both cell types showed good biocompatibility in GelMA. Lipopolysaccharide (LPS) was added to the cell models to create inflammation models, which resulted in increased expression of inflammatory factors IL-1 β , TNF- α , iNOS, and IL-6, and decreased expression of cell functional genes such as Collagen II (COLII), transcription factor SOX-9 (Sox9), Aggrecan, alkaline phosphatase (ALP), RUNX family transcription factor 2 (Runx2), Collagen I (COLI), Osteopontin (OPN), and bone morphogenetic protein-2 (BMP-2). The created inflammation model was then used to evaluate the effectiveness of Dangguinantongtang (DGNT) decoctions. The results showed that DGNT reduced the expression of inflammatory factors and increased the expression of functional genes in the cell model. In summary, this study established a 3D cell model to assess the effectiveness of traditional Chinese medicine (TCM) decoctions, characterized the gene expression profile of the inflammatory state model, and provided a practical reference for future research on TCM efficacy evaluation for arthritis treatment.

Keywords 3D bioprinting, Chondrocytes, Osteoblasts, Arthritis, Decoction

[†]Zhichao Liang, Yunxi Han and Tao Chen have equally contributed to this work.

*Correspondence:

Yang Liu

lyshtcm@126.com

Lianbo Xiao

13701888178@163.com

Qianqian Liang

liangqianqiantcm@126.com

¹ Longhua Hospital, Shanghai University of Traditional Chinese Medicine, 725 Wan-Ping South Road, Shanghai 200032, China

² Guanghua Hospital Affiliated to Shanghai University of Traditional Chinese Medicine, 540 Xinhua Road, Shanghai 200052, China

³ Spine Institute, Shanghai University of Traditional Chinese Medicine, 725 Wan-Ping South Road, Shanghai 200032, China

⁴ Key Laboratory of Theory and Therapy of Muscles and Bones, Ministry of Education (Shanghai University of Traditional Chinese Medicine), 1200 Cailun Road, Shanghai 201203, China

⁵ Institute of Arthritis Research in Integrative Medicine, Shanghai Academy of Traditional Chinese Medicine, 540 Xinhua Road, Shanghai 200052, China

⁶ Shanghai Key Laboratory of Orthopaedic Implant, Department of Orthopaedic Surgery, Shanghai Ninth People's Hospital Affiliated Shanghai Jiao Tong University School of Medicine, 639 Zhizaoju Rd, Shanghai 200011, China

⁷ Institute of Rehabilitation Medicine, School of Rehabilitation Science, Shanghai University of Traditional Chinese Medicine, Engineering Research Center of Traditional Chinese Medicine Intelligent Rehabilitation, Ministry of Education, 1200 Cailun Road, Shanghai 201203, China

⁸ Department of Oral & Cranio-Maxillofacial Surgery, Shanghai Ninth People's Hospital, College of Stomatology, Shanghai Jiao Tong University School of Medicine, 639 Zhizaoju Rd, Shanghai 200011, China



Introduction

Arthritis is an inflammatory disease that affects the joints in the limbs and the surrounding tissues. It is a major source of pain, disability, and socioeconomic costs globally. In patients with arthritis, various tissues are stimulated by inflammation and secrete high levels of inflammatory factors and matrix metalloproteinases (MMPs). This leads to massive matrix loss and excessive apoptosis of chondrocytes and osteoblasts, ultimately resulting in joint destruction and deformity. Nonsteroidal anti-inflammatory drugs (NSAIDs) and glucocorticoids are widely recognized as the primary pharmacological interventions for the treatment of arthritis [1]. The NSAIDs have the propensity to induce adverse reactions within the digestive, cardiovascular, and renal systems [2]. Furthermore, prolonged administration of glucocorticoids is associated with an increased susceptibility to hypertension, osteoporosis, and various other metabolic disorders [3, 4]. Despite the extensive clinical use of Danguiniantong (DGNT) decoctions in China for the treatment of arthritis for thousands of years, there is limited scientific research to validate their therapeutic efficacy.

Relying solely on the conventional two-dimensional (2D) cell culture model for drug screening has shown limitations in achieving satisfactory *in vivo* and clinical efficacy for the screened drugs. This approach has been the prevailing method for a significant period of time, but its effectiveness has been questioned. Therefore, it is necessary to explore alternative models for drug screening. The scientific community is increasingly emphasizing and acknowledging the crucial role of the extracellular matrix (ECM) in governing cell behavior [5]. In order to achieve a more accurate representation of the conditions present within living organisms, extensive advances have been made in the field of three-dimensional (3D) cell culture techniques. 3D cultures offer a more accurate and in-depth portrayal of organismal conditions *in vitro* by faithfully replicating the intercell and ECM signaling microenvironment [6, 7].

This disparity is evident at the gene and protein expression levels [8]. 3D models are now extensively utilized in the study of various diseases, including lung cancer [9], breast cancer [10], retinal glial cells [11] and skeletal muscle [12]. However, the availability of 3D models specific to joints is still relatively limited. Currently, most studies of 3D printed joint scaffold models focus on tissue engineering for articular cartilage repair [13–16]. There are very few *in vitro* models targeting the assessment of drug efficacy in arthritis [17, 18]. *In vitro* models for efficacy studies of herbal decoction are not yet available.

ATDC5 and MC3T3-E1 cells are widely used in arthritis research. Many studies have shown that LPS can

induce inflammatory factor expression in ATDC5 cells [19–21], and induces the down-regulation of functional genes in MC3T3-E1 cells [22, 23]. This study aimed to establish a 3D cell model using methacryloyl gelatin (GelMA) that accurately replicates the inflammatory conditions of ATDC5/MC3T3-E1 cells. The pioneering model was developed to evaluate the therapeutic efficacy of Traditional Chinese medicine (TCM) decoctions in the treatment of arthritis. Initially, the biocompatibility of the model used in this study was assessed, followed by the observation of gene expression in ATDC5/MC3T3-E1 cells under inflammatory conditions. Subsequently, the model was used as a platform to evaluate the anti-inflammatory properties of DGNT decoctions. The findings collectively confirmed the 3D model that effectively validates the effectiveness of TCM decoctions in treating arthritis.

Materials and methods

Cells culture

The ATDC5 and MC3T3-E1 cell lines were obtained from the prestigious Cell Bank of the Chinese Academy of Sciences (Shanghai, China). The complete medium for ATDC5 cell line comprised DMEM/F12 supplemented with 10% fetal bovine serum and 1% penicillin–streptomycin solution. The complete culture medium required for the MC3T3-E1 cell line consisted of α -MEM supplemented with 10% fetal bovine serum and 1% Penicillin–streptomycin solution.

Bioink

The materials GelMA and Lithium phenyl-2,4,6-trimethylbenzoylphosphinate (LAP) were procured from EFL-Tech Co., Ltd. (Suzhou, China). 5% (w/v) of GelMA and 0.25% (w/v) of LAP were solubilized in PBS to prepare the hydrogel solution. The solution thus obtained was sterilized in a 60 °C oven for one hour and later stored in a 37 °C incubator. Subsequently, ATDC5/MC3T3-E1 cells were added to the prepared hydrogel solution at a concentration of 2×10^6 /ml. This mixture constituted the bioink used in this study.

The preparation process of the 3D cell model

The 3D printing of the cell model was carried out using a 3D printer manufactured by Regenovo Biotechnology Co. Ltd. Detailed parameters for the printing programs are provided as follows: temperature control set to 20 °C, model layer thickness of 0.3 mm, with a total number of 4 layers. The height of each individual layer was set to 1.2 mm, while the total height of the model measured 2 mm, width measured 6.5 mm \times 6.5 mm. Following the printing process, the bioink was exposed to UV light for a duration of 10–15 s to achieve instant solidification.

CCK-8 assays

To evaluate cell proliferation, the CCK-8 assay (Dojindo, Shanghai, China) was performed using the respective CCK-8 kit. Following the culture of 3D cell constructs for assorted durations in 48-well plates, the CCK-8 assay solution was introduced, and the resultant enzymatic marker was assessed for its corresponding OD value.

Live/dead staining

The 3D cell constructs were seeded into 48-well plates. Staining reagents were added on day 1, day 2, day 4, day 7 and day 10 according to kit instructions (Sigma), and cells growth was observed using a fluorescent microscope.

Detection of alkaline phosphatase (ALP) activity

The ALP staining kit was purchased from Shanghai Beyotime Biotechnology Co., Ltd. Cells or 3D cell models were treated with Western and IP cell lysates (3D printed models were homogenized by adding grinding beads). Add the samples to 96-well plates and measure the absorbance following the instructions provided in the kit.

Drug administration

The herbal medicines used to prepare the DGNT decoctions were obtained from the Longhua Hospital, which is affiliated with the Shanghai University of Traditional Chinese Medicine. The herb dosage was converted using a conversion factor of 9.01. The concentration of the herb after the decoctions was determined to be 1.89 g/ml. The preparation of the DGNT decoctions involved 15 types of herbs, as shown in Table 1. To prepare the DGNT

decoctions lyophilized powder, the prepared decoctions were centrifuged, and the resulting supernatant was filtered and then stored at -80°C . It was further lyophilized in a vacuum dryer for 48–72 h and stored at -80°C . For the in vitro experiments, the lyophilized powder was dissolved in complete medium, filtered using a $0.22\ \mu\text{m}$ filter, and subsequently used.

Quantitative RT-PCR

Cells were harvested, and cDNA was generated using Trizol (Invitrogen) and PrimeScript™ RT reagent Kit (cat. #RR037A). The gene expression was quantified by RT-PCR using QuantiTect SYBR Green (Hieff-TM). The primers for qPCR are shown in Table 2. All

Table 1 The composition of DGNT decoctions

Latin name	Chinese name of medicine	Dosage, g
<i>Notopterygium incisum</i>	Qiang Huo	15
<i>Rhizoma Cimicifugae</i>	Sheng Ma	3
<i>Atractylodes macrocephala</i>	Bai Shu	3
<i>Angelica sinensis</i> (Oliv.) Diels	Dang Gui	9
<i>Glycyrrhiza uralensis</i> Fisch	Gan Cao	15
<i>Scutellaria baicalensis</i> Georgi	Huang Qin	3
<i>Artemisiacapillaris</i> Thunb	Yin Chen	15
<i>Anemarrhena asphodeloides</i> Bunge	Zhi Mu	9
<i>Saposhnikovia divaricata</i>	Fang Feng	9
<i>Puerariae Lobatae Radix</i>	Ge Gen	6
<i>Atractylodes lan cea</i>	Cang Shu	9
<i>Panax ginseng</i> C. A. Mey	Ren Shen	6
<i>Sophora flavescens</i>	Ku Shen	6
<i>Alisma plantago-aquatica</i> Linn	Ze Xie	9
<i>Polyporus</i>	Zhu Ling	9

Table 2 Primer sequence for RT-PCR

Gene	5' to 3'
COLI	F: CTTTGCTTCCCAGATGTCCT R: CGGTGTCCTTCATCCAG
COLII	F: ACCTTGGACGCCATGAAA R: CAGGGCAGTGTATGTGAACC
IL-6	F: TGCCTTCTGGGACTGAT R: TTGCCATTGCACAACCTCTT
iNOS	F: GAGCGAGTTGTGGATTGTC R: CCAGGAAGTAGGTGAGGG
MMP13	F: GCAGTTCCAAAGGCTACA R: CTCGGAGACTGGTAATGG
Sox9	F: AGTACCCGCATCTGCACAAC R: ACGAAGGGTCTCTCTCGCT
IL-1 β	F: CTGGTACATCAGCACCTCAC R: AGAAACAGTCCAGCCCATAC
TNF- α	F: AGTGACAAGCCTGTAGCCC R: GAGGTTGACTTTCTCTGGTAT
ALP	F: AACAACTGACTGACCCCTTC R: ATCCTGCCTCCTTCCACTA
Runx2	F: AACTTCCTGTGCTCCGTGCTG R: TCGTTGAACCTGGCTACTTGG
Osterix	F: AGGAGGCACAAGAAGCCATACC R: ATGCCTGCCTTGTACCACGAGC
OCN	F: GGACCATCTTCTGTCTCACTCTG R: GTTCACTACTTATTGCCCTCCTG
OPN	F: CCAGCAGCAGGACTGAAGGAGC R: TTCACCGGAGACAGGAGGC
BMP-2	F: CAACACCGTTCAGCTTCC R: TTCCCACTCATTTCTTCC
Aggrecan	F: GACTGTCTATCTACACGCCAACCA R: GATGTCGTCTTACCACCCAC
β -Actin	F: GGTGGGAATGGGTGAGAAGG R: GTTGGCCTTAGGGTTCAGGG

F, forward; R, reverse

primers were purified and synthesized by the Huada Company (HuaDa, Shenzhen, China).

Statistical analysis

Statistical analyses were performed with GraphPad Prism 9.0 software. Data are presented as mean \pm SEM. Analyses between 2 groups used unpaired Student t-test. When comparing the difference among >2 groups, one-way ANOVA analysis of variance was used followed by a Tukey multiple comparisons posttest. *P* values < 0.05 were considered statistically significant.

Results

The design of the 3D cell model

Regenovo Bio-3D printers offer design pathways and printing functions, guaranteeing reasonable porosity and consistent printing performance (Fig. 1).

The excellent biological characterization of the 3D cell model

The schematic diagram showed in Fig. 2A depicts the construction process of the ATDC5 cells model and the corresponding biological studies. ATDC5-containing hydrogel scaffolds were cultured for 1, 2, 4, 7, and 10 days, followed by live/dead cells staining. Analysis of the results demonstrated that the survival rate of ATDC5 cells within the 3D model exceeded 90% (Fig. 2B, C). The cell activity assay using CCK-8 was conducted, and the hydrogel scaffolds containing ATDC5 demonstrated notable proliferative activity compared to the blank scaffold group (Fig. 2D). It is important to identify and analyze specific marker genes in order to understand the functional traits and properties of chondrocytes. In contrast to the conventional 2D culture of ATDC5 cells, our

3D cell model exhibited a significant upregulation in the expression of the functional gene Collagen II (COLII) mRNA, with a 1.5-fold increase on day 7 (Fig. 2E). Moreover, the expression of Aggrecan mRNA exhibited a remarkable 4.5-fold increase on day 7 (Fig. 2F), while the expression of transcription factor SOX-9 (Sox9) mRNA demonstrated an even greater increase of fivefold (Fig. 2G).

The schematic diagram showed in Fig. 3A depicts the construction process of the MC3T3-E1 cell model and the corresponding biological studies. MC3T3-E1-containing hydrogel scaffolds were cultured for varying durations of 1, 2, 4, 7, and 10 days. Afterward, they were subjected to live/dead cell staining. Analysis of the obtained results revealed that the survival rate of MC3T3-E1 cells within the 3D model surpassed 90%, as depicted in Fig. 3B–C. The CCK-8 assay was performed to assess cell activity, where the hydrogel scaffolds containing MC3T3-E1 cells exhibited a significant increase in proliferative activity compared to the blank scaffold group, as illustrated in Fig. 3D. Quantification of ALP activity in MC3T3-E1 cells revealed a noteworthy increase within the 3D model compared to the conventional 2D culture. Specifically, ALP activity within the 3D model was twofold higher on day 14 and reached a threefold increase on day 21, as depicted in Fig. 3E. RT-PCR analysis of MC3T3-E1 cells revealed distinct differences in gene expression profiles between the 3D model and the conventional 2D culture. In the MC3T3-E1 cell 3D model, ALP mRNA expression was twofold higher than in the 2D culture on day 7 and nearly fourfold higher on day 14. Similarly, the expression of Collagen I (COLI) mRNA showed a twofold increase on day 14. However, there was no significant difference

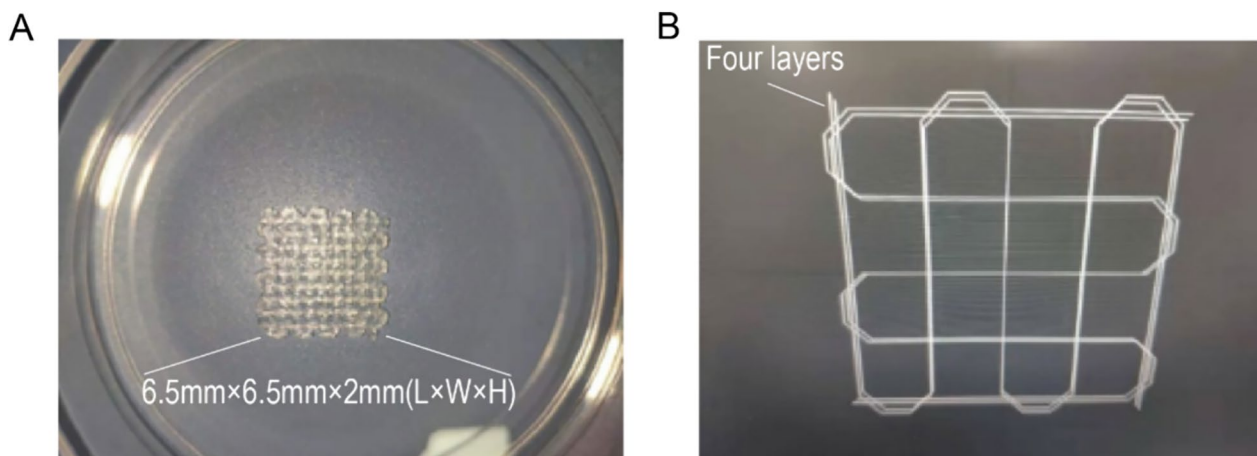


Fig. 1 The design of a 3D cell model. **A** 3D printed cell model samples. The height of each individual layer was set to 1.2 mm, while the total height of the model measured 2 mm, width measured 6.5 mm \times 6.5 mm. **B** 3D printing design path of the scaffold. The printing programs are provided as follows: temperature control set to 20 $^{\circ}$ C, model layer thickness of 0.3 mm, with a total number of 4 layers

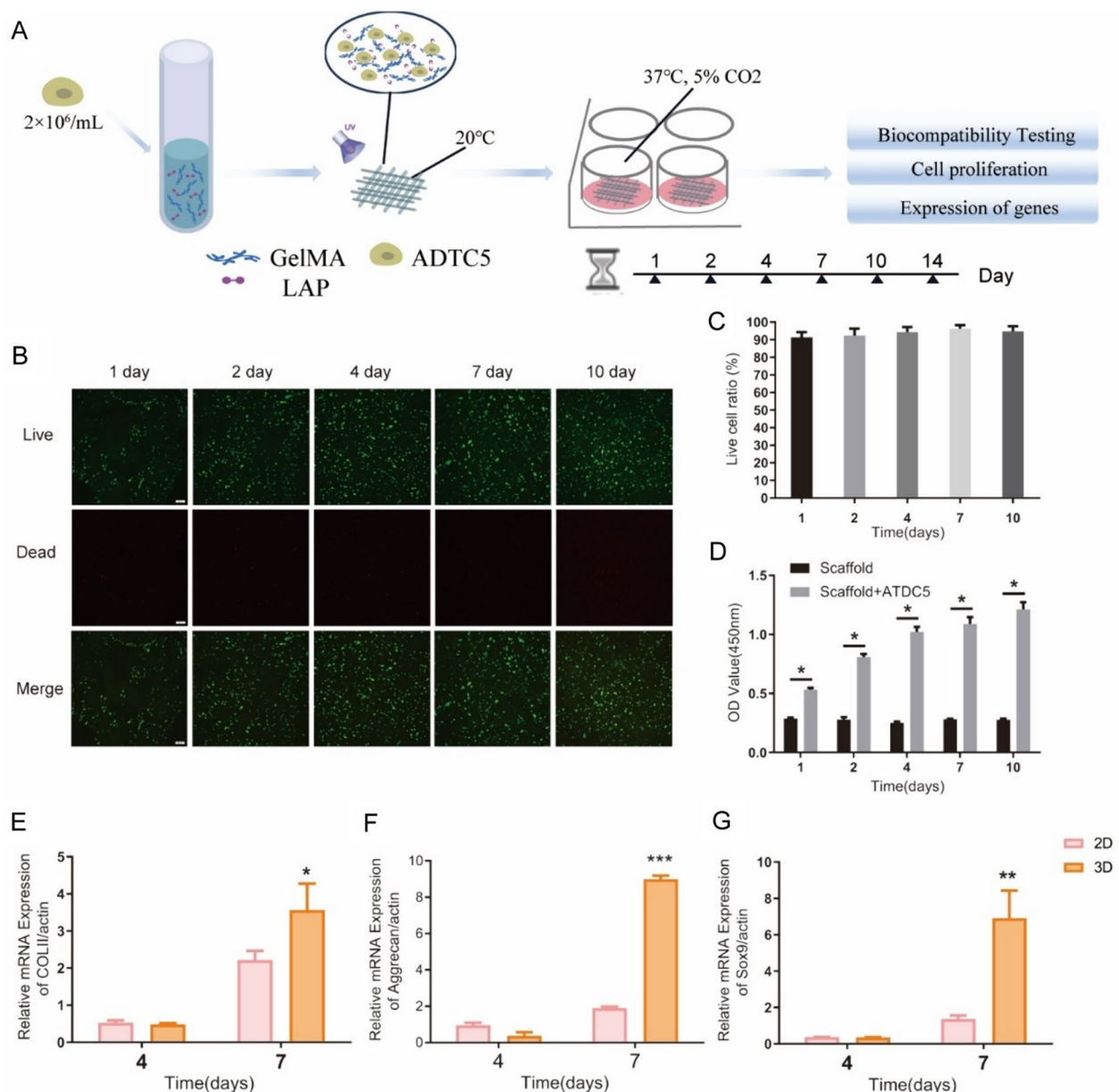


Fig. 2 Biological characterization of the ATDC5 cell model. **A** Schematic diagram of the experimental. **B** ATDC5 Cell were stained using the LIVE/DEAD Cell Viability/Cytotoxicity Assay Kit, with green fluorescence indicating live cells and red fluorescence indicating dead cells. **C** The survival rate of cell in 3D cell model after various days of culture is shown ($n=6$). **D** Cell proliferation was analyzed using the CCK-8 assay ($n=5$, t-test, $*P<0.05$). **E–G** RT-PCR assay was performed to analyze the mRNA expression of COL1I, Sox9 and Aggrecan in ATDC5 cells ($n=5$, t-test, $*P<0.05$, $**P<0.01$, $***P<0.001$ VS. 2D group)

in the expression of RUNX family transcription factor 2(Runx2) mRNA compared to the control 2D culture (Fig. 3F–H).

Construction of 3D cell model in LPS-induced inflammatory state

The process of stimulating the 3D cell model (ATDC5) with lipopolysaccharide (LPS) is depicted in Fig. 4A.

The CCK-8 assay was used to evaluate the impact of LPS on cell activity within a 3D model of ATDC5 cells. The results showed significant inhibition of activity at a concentration of $50 \mu\text{g/ml}$ (Fig. 4B). The investigation further revealed that LPS stimulation negatively influenced the gene expression of ATDC5 cells. The analysis of RT-qPCR indicates a significant upregulation in the expression of inflammatory mediators such as $\text{IL-1}\beta$,

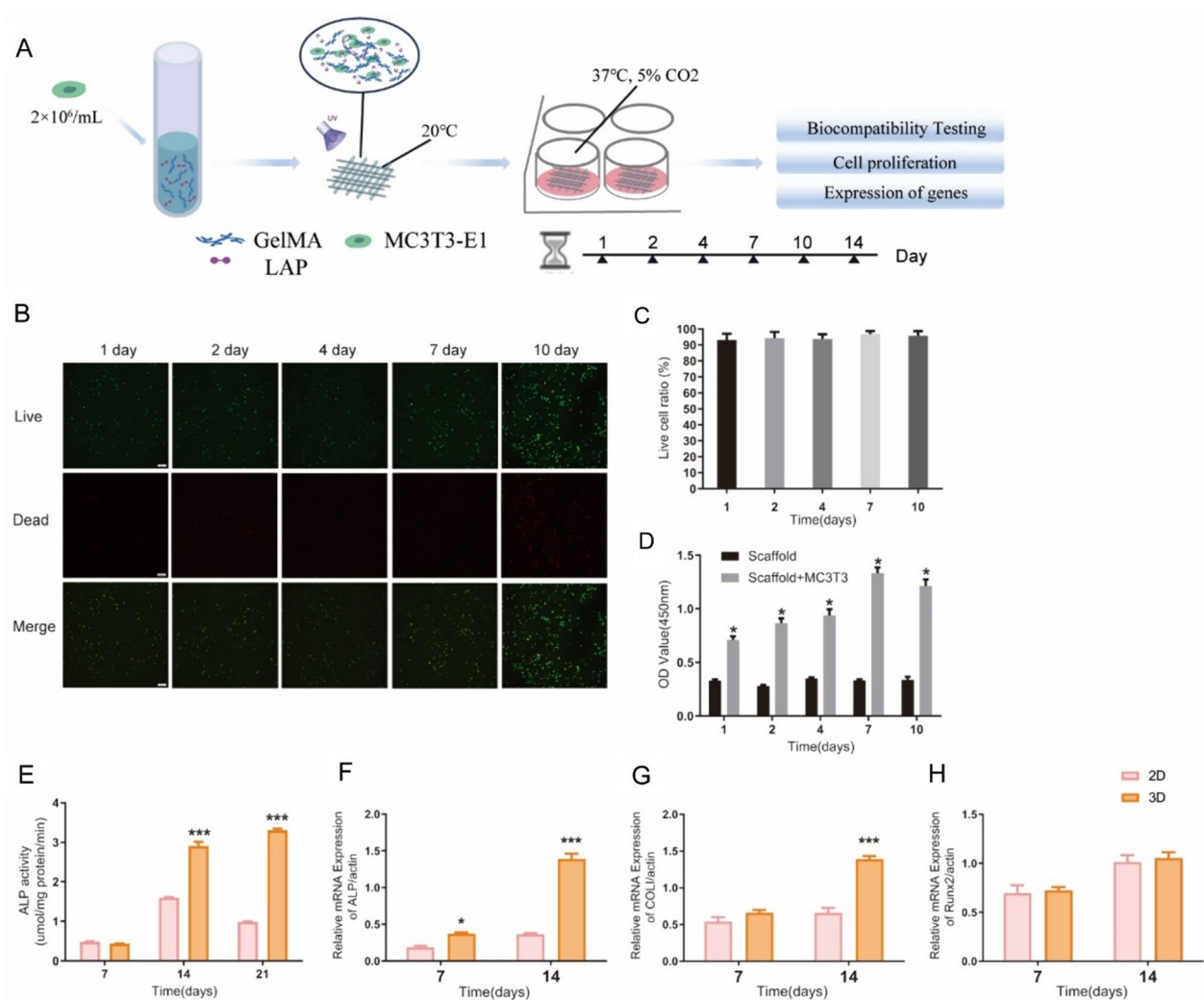


Fig. 3 Biological characterization of the MC3T3-E1 cell model. **A** Schematic diagram of the experimental. **B** MC3T3-E1 Cell were stained using the LIVE/DEAD Cell Viability/Cytotoxicity Assay Kit, with green fluorescence indicating live cells and red fluorescence indicating dead cells. **C** The survival rate of cells in 3D cell model after various days of culture is shown (n=6). **D** Cell proliferation was analyzed using the CCK-8 assay (n=5, t-test, *P<0.05). **E** Alkaline phosphatase activity assay of MC3T3-E1 cells (n=5, t-test, ***P<0.001 VS. 2D group). **F–H** RT-PCR assay was performed to analyze the mRNA expression of ALP, COL1 and Runx2 in MC3T3-E1 cells (n=5, t-test, *P<0.05, ***P<0.001 VS. 2D group)

IL-6, TNF- α , and iNOS after LPS treatment in the 3D model of ATDC5 cells (Fig. 4C–F). Concurrently, a substantial decrease was observed in the expression of COLII, Aggrecan, and Sox9 (Fig. 4G–I). Moreover, LPS stimulation elicited an increased expression of matrix metalloproteinase 13 (MMP13) (Fig. 4J).

The process of stimulating the 3D cell model (MC3T3-E1) with lipopolysaccharide (LPS) is depicted in Fig. 5A. The CCK-8 assay showed that LPS inhibited cell activity in the 3D model of MC3T3-E1 cells (Fig. 5B) at a 5 μ g/ml concentration. In the 3D model of MC3T3-E1 cells, LPS stimulation resulted in decreased expression of functional genes ALP, Runx2, COLI,

Osterix, Osteocalcin (OCN), Osteopontin (OPN), and bone morphogenetic protein-2(BMP-2) (Fig. 5C–I).

DGNT attenuates inflammation and promotes bone formation in cell models of inflammatory states

The experimental procedure of DGNT affecting 3D cell models (ATDC5) in inflammatory states was depicted in a schematic diagram (Fig. 6A). The cytotoxicity of the drug was assessed using the ATDC5 cell model. The ATDC5 cells were treated with DGNT for 24 h, and cell viability was evaluated using CCK-8. It was observed that DGNT at concentrations of 200 μ g/ml, 500 μ g/ml, 1000 μ g/ml and 2000 μ g/ml had minimal effect on the ATDC5 cell model (Fig. 6B). A concentration-dependent

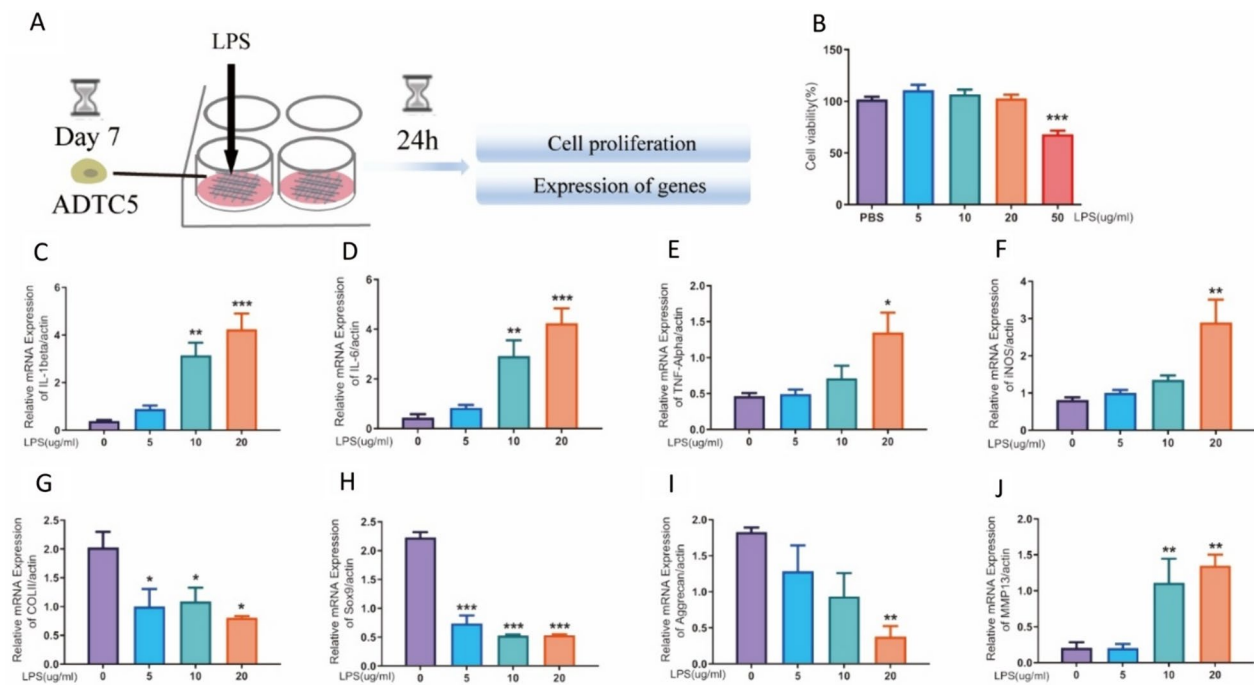


Fig. 4 The expression of genes associated with the ATDC5 3D cell model was changed by distinct concentrations of lipopolysaccharide (LPS). **A** Schematic diagram of the experimental. **B** Effect of LPS on the cell activity of ATDC5 cells ($n=5$, one way ANOVA, $***P < 0.001$ VS. PBS group). **C–F** The mRNA expression of inflammatory factors (IL-1 β , IL-6, TNF- α , and iNOS) under the LPS-induced inflammatory state ($n=3$, one way ANOVA, $*P < 0.05$, $**P < 0.01$, $***P < 0.001$ VS. PBS group). (G–J) The mRNA expression of functional genes (COLII, Sox9, Aggrecan and MMP13) under the LPS-induced inflammatory state ($n=3$, one-way ANOVA, $*P < 0.05$, $**P < 0.01$, $***P < 0.001$ VS. PBS group)

inhibitory effect on IL-1 β , IL-6, TNF- α , and iNOS in the 3D model of ATDC5 cell was observed in the RT-qPCR results, indicating the suppressing inflammation properties of the DGNT (Fig. 6C–F). Furthermore, the expression of functional genes, including Aggrecan, COLII, and Sox9, were upregulated, while the expression of MMP13 was downregulated in response to the DGNT treatment (Fig. 6G–J).

The experimental procedure of DGNT affecting 3D cell models (MC3T3-E1) in inflammatory states was depicted in a schematic diagram (Fig. 7A). The 3D model of MC3T3-E1 cell was intervened with DGNT for 24 h, and cell viability was assessed using the CCK8 assay. It was observed that DGNT, at concentrations of 200 $\mu\text{g/ml}$, 500 $\mu\text{g/ml}$, 1000 $\mu\text{g/ml}$, and 2000 $\mu\text{g/ml}$, had a negligible impact on the cell activity of the MC3T3-E1 3D model (Fig. 7B). RT-PCR analysis revealed that DGNT concentration-dependently enhanced the expression of ALP, Runx2, COLI, Osterix, OCN, OPN, and BMP-2 (Fig. 7C–I).

Discussion

In this study, a 3D cell model of ATDC5/MC3T3-E1 cells and an inflammation model were constructed. We constructed a preliminary 3D cell model. On this model

we can use LPS to induce a simple inflammatory osteoblast/chondrocyte model. The various types of arthritis have different characteristics, they all show a pathological process of inflammatory infiltration of bone and cartilage during their development. Rather than looking at a specific type of arthritis, we have focused on bone and cartilage damage. By comparison, it was found that the expression of inflammatory factors in ATDC5 cells was up-regulated in the model, which is consistent with existing studies. The down-regulation of functional genes, such as COLII, Runx2, and ALP in ATDC5/MC3T3-E1 cells is consistent with previous studies [24–27]. We found that the normal 3D model exhibited excellent biological effects in the absence of LPS stimulation. In 3D cellular inflammation models, LPS needs to be used at double or even higher doses to achieve the desired inflammation induction [19, 28–33]. The cause of the discrepancy may be related to the bioink, but we prefer to attribute it to the spatial distribution of cells. DGNT decoctions reduced the expression of inflammatory factors in vitro, which is consistent with previous efficacy studies of DGNT decoctions [34, 35]. The ability of DGNT decoctions to enhance the expression of functional genes aligns with the findings of other studies on drugs targeting genes that enhance osteoblast function

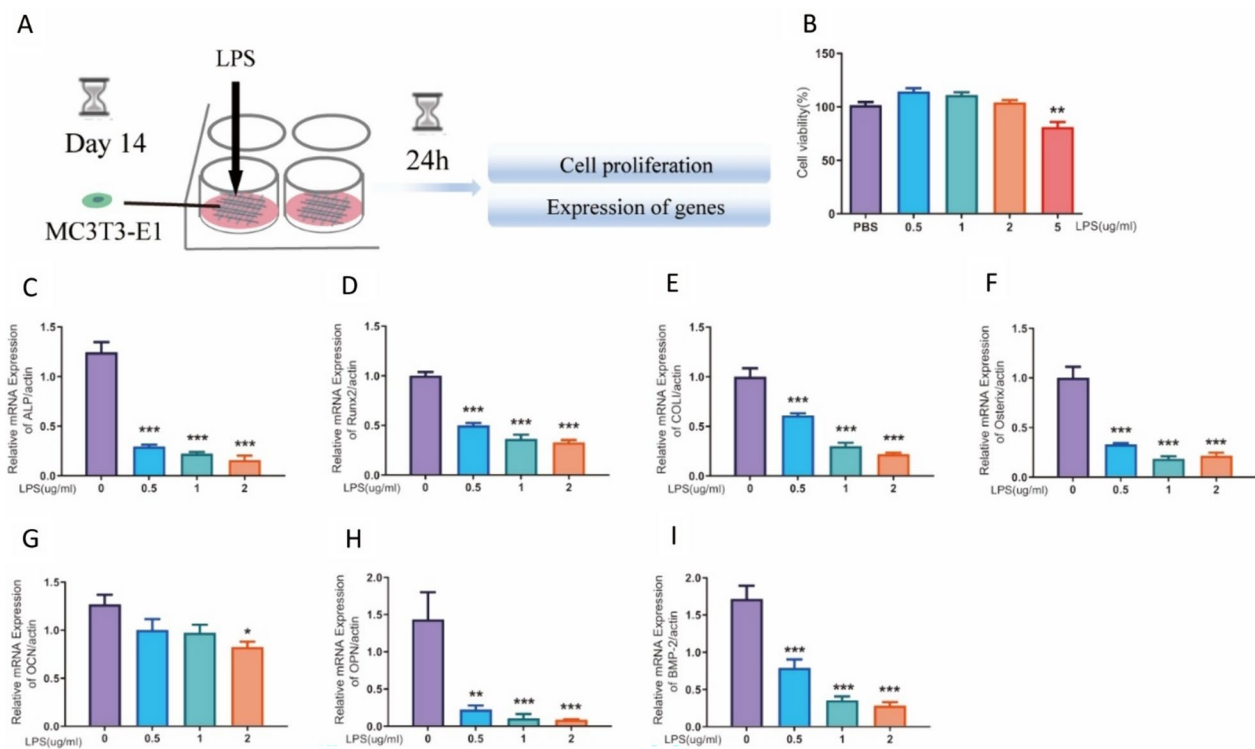


Fig. 5 The expression of genes associated with the MC3T3-E1 3D cell model was changed by distinct concentrations of LPS. **A** Schematic diagram of the experimental. **B** Effect of LPS on the cell activity of MC3T3-E1 cells ($n=5$, one way ANOVA, $**P < 0.01$ VS. PBS group). **C–I** The mRNA expression of functional genes (ALP, Runx2, COL1, Osterix, OCN, OPN, and BMP-2) under the LPS-induced inflammatory state. ($n=3$, one-way ANOVA, $*P < 0.05$, $**P < 0.01$, $***P < 0.001$ VS. PBS group)

[36–38]. The experimental results suggest that these 3D cell models can be used to assess the efficacy of TCM decoctions.

In conventional 2D cell culture models, cells are restricted to adhering to the substrate in contact with the culture surface [5, 39]. Hydrogel scaffolds provide a 3D structure that more closely resembles in vivo tissues [40, 41], in 3D culture, cells are capable of adhering to the culture surface in a more widespread manner. 3D culture helps maintain the morphology and function of osteoblasts/chondrocytes [42]. The degree of cells adhesion and stretching can impact crucial functions related to proliferation, apoptosis, and differentiation. The morphology of cells growth becomes more diverse in 3D model culture and resembles the diversity in vivo tissues [39, 43, 44]. Additionally, physiological interactions between cells and the ECM are replicated in a 3D model culture, which more accurately mimics the growth environment within the body [45, 46]. Compared to 2D cell culture, 3D model culture better simulate signaling between cells. This is important for studying cellular

molecular pathways and signaling involved in the development of arthritis.

Although the application of 3D cell model to arthritis drug screening is in its early stages, several studies have researched their potential advantages. Researchers chose chondrocytes [47–50], synovial fibroblasts [51], RA fibroblast-like-synoviocytes [52] and vascular endothelial cells [51] as the research subjects in the constructed models, based on the pathological characteristics of different types of arthritis. Of particular interest is the fact that the vast majority of researchers chose to simulate the 3D state by culturing the cells in a hydrogel matrix without using 3D printing technology. Compared to cells cultured within a 3D matrix gel system, implementing 3D printed scaffolds offers a clear advantage in providing cells with a spatial structure. The strategies employed by the researchers to induce inflammation varied in their approaches to modeling inflammatory activation. Y [47] and Satyavrata Samavedi [49] chose to use co-culture with macrophages activated by LPS as an inflammatory activation condition. However, Lin [51] and Rosser

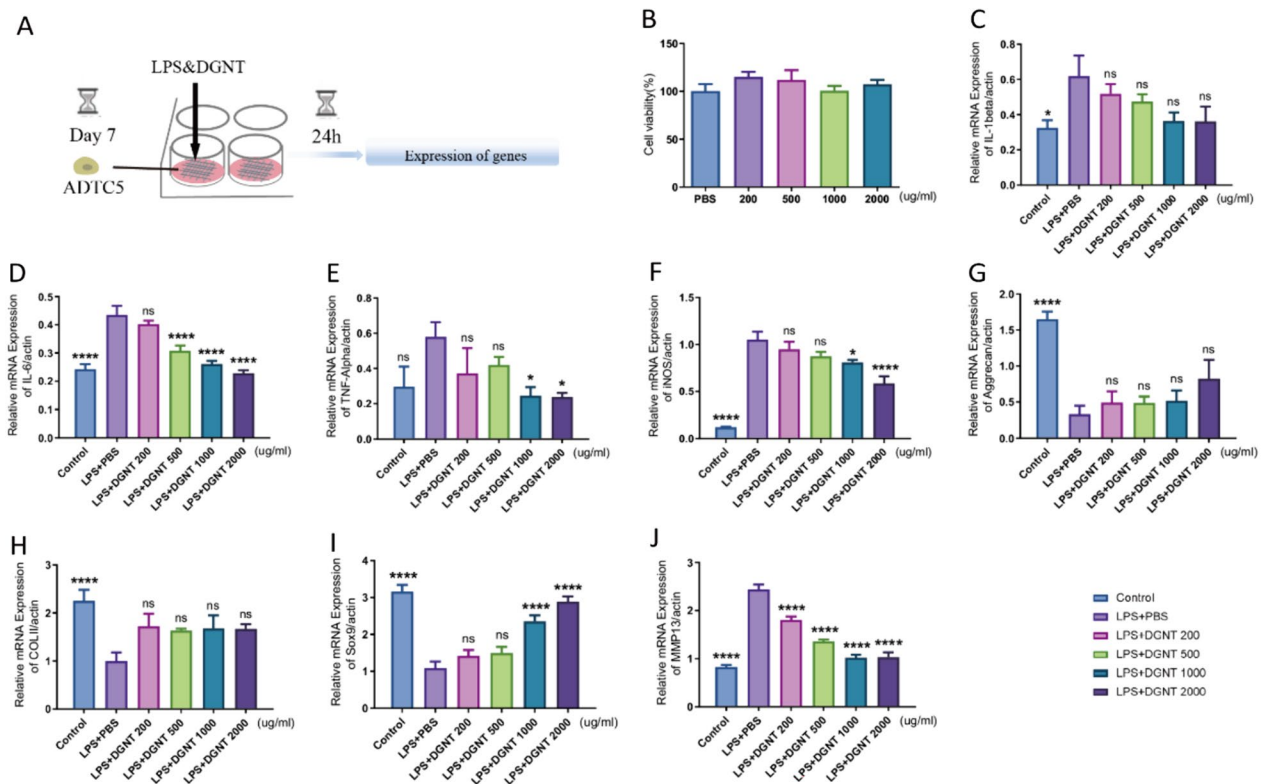


Fig. 6 DGNT has reduced inflammation caused by LPS in ATDC5 cell and increased the expression of relevant functional genes. **A** Schematic diagram of the experimental. **B** Effect of DGNT on the activity of ATDC5 cell models. **C–F** LPS-induced mRNA expression of inflammatory factors (IL-1 β , IL-6, TNF- α , and iNOS) in response to DGNT intervention (n = 10, one way ANOVA, * P < 0.05, **** P < 0.0001 VS. LPS + PBS group). **G–J** LPS-induced mRNA expression of functional genes (Aggrecan, COL11, Sox9 and MMP13) in the inflammatory state under DGNT intervention (n = 10, one-way ANOVA, **** P < 0.0001 VS. LPS + PBS group)

[48] used cytokines such as TNF- α , Li [50] used IL-1 β . The utility in assessing the efficacy of herbal decoctions, which has not been reported in other studies. It is worth mentioning that the 3D model is easy to construct, has a low construction cost, and can be reproduced easily. This makes it, which provides a valuable and practical reference for research in this field. In most studies of arthritis, the TNF- α gene is overexpressed under inflammatory conditions [21, 53, 54]. In the 3D cellular inflammation model of this study, ATDC5 cells had elevated TNF- α gene expression (Fig. 4E).

While the current study has provided significant findings, it is essential to acknowledge certain limitations. Notably, LPS, a constituent of the outer membranes of

gram-negative bacteria, can induce inflammation and impair the functioning of osteoblasts and chondrocytes in cell cultures [23, 55, 56]. Therefore, we have prioritized using LPS as the stimulus, acknowledging its singular but essential role. However, it is worth noting that future investigations could also explore alternative stimulation modalities, such as TNF- α or IL-1 β . Due to the disparities in the culture conditions utilized for ATDC5 cells and MC3T3-E1 cells, it was not feasible to achieve a mixed culture of these cell types under inflammation-inducing conditions. Consequently, we were unable to establish a hybrid model with our current efforts. However, this will be a crucial aspect of our future research endeavors.

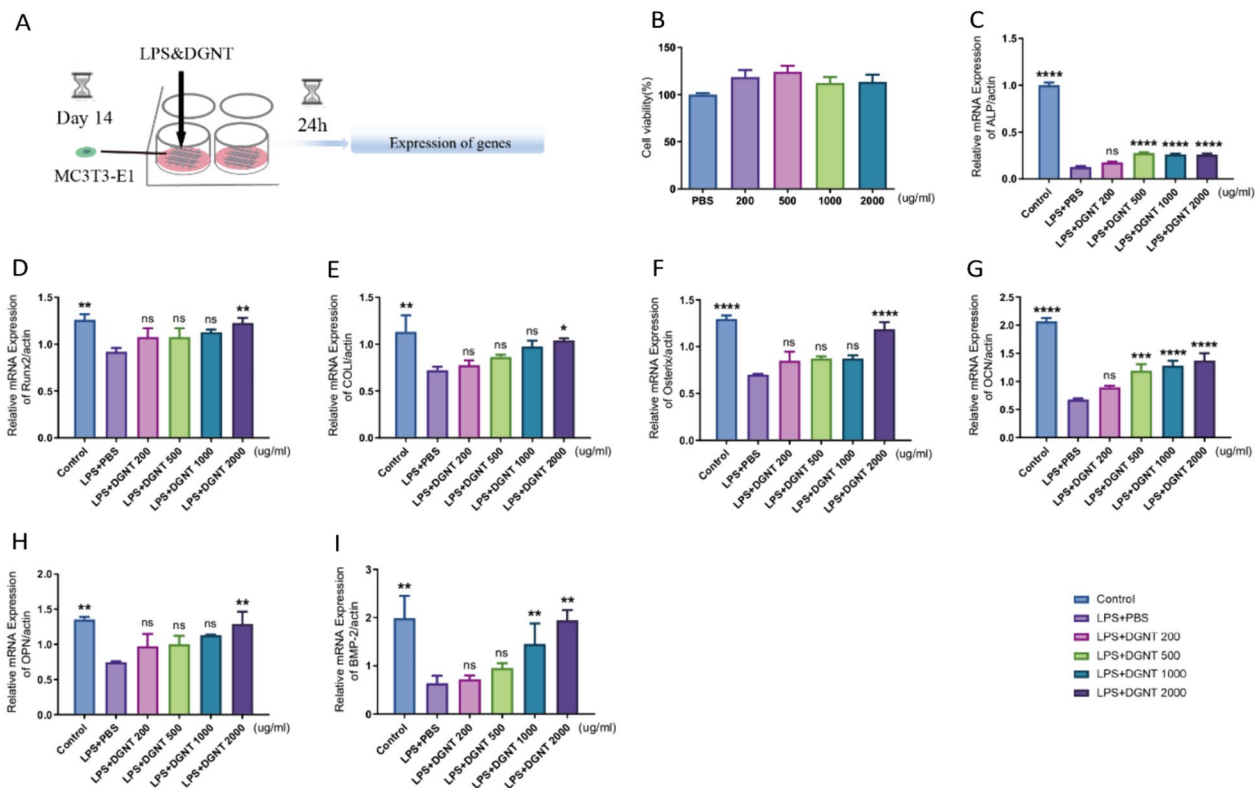


Fig. 7 DGNT enhanced functional gene expression in MC3TE-E1 cell under LPS stimulation. **A** Schematic diagram of the experimental. **B** Effect of DGNT on the activity of MC3T3-E1 cell model. **C–I** mRNA expression analysis of essential functional genes (ALP, Runx2, COLI, Osterix, OCN, OPN and BMP-2) under LPS-induced inflammatory conditions, with intervention by DGNT (n = 10, one-way ANOVA, **P* < 0.05, ***P* < 0.01, ****P* < 0.001, *****P* < 0.0001 VS. LPS + PBS group)

Conclusion

In this study, our utilization of 3D printing technology allowed us to create a model of joint inflammation, which enabled us to objectively assess the potential therapeutic effects of herbal decoctions. Our results revealed that the ATDC5/MC3T3-E1 cells exhibited enhanced viability and functionality when seeded in scaffolds, as opposed to conventional 2D cultures. Moreover, our study revealed the anti-inflammatory effects demonstrated by the DGNT in our inflammation model. Crucially, our research holds essential implications as it provides a valuable reference and establishes the foundation for integrating 3D printing technology in investigating the therapeutic effectiveness associated with traditional Chinese medicine decoctions.

Abbreviations

ALP	Alkaline phosphatase
BMP-2	Bone morphogenetic protein-2
COLI	Collagen I
COLII	Collagen II
DGNT	Danguinantongtang
ECM	Extracellular matrix
GelMA	Methacryloyl gelatin

LPS	Lipopolysaccharide
LAP	Lithium phenyl-2,4,6-trimethylbenzoylphosphinate
MMPs	Matrix metalloproteinases
MMP13	Matrix metalloproteinase 13
NSAIDs	Nonsteroidal anti-inflammatory drugs
OCN	Osteocalcin
OPN	Osteopontin
Runx2	RUNX Family Transcription Factor 2
Sox9	Transcription factor SOX-9
TCM	Traditional Chinese medicine
3D	Three-dimensional
2D	Two-dimensional

Acknowledgements

Not applicable.

Author contributions

Zhichao Liang: conceptualization, methodology, software, validation, formal analysis, investigation, resources; Yunxi Han: software, formal analysis, writing—original draft; Tao Chen: software, validation, formal analysis, writing—review & editing; Jinwu Wang: Methodology; Kaili Lin: methodology; Luying Yuan: resources; Xuefei Li: resources; Hao Xu: methodology; Tengting Wang: formal analysis, Resources; Yang Liu: conceptualization, methodology, software, validation, investigation, writing—original draft; Lianbo Xiao: conceptualization, methodology, supervision; Qianqian liang: conceptualization, methodology, writing—review & editing, supervision, project administration, funding acquisition.

Funding

This work was sponsored by research grants from National Natural Science Foundation (81920108032, 81822050), State Administration of Traditional Chinese Medicine Young Qi Huang Scholar, New interdisciplinary research Project of Shanghai Municipal Health Commission (2022JC005), Innovation team project of scientific research of traditional Chinese medicine of Shanghai Health Committee (2022CX001), Shanghai "Science and Technology Innovation Action Plan" Medical Innovation Research Special Project (21Y11921400), Shanghai TCM Medical Center of Chronic Disease (2022ZZ01009), Shanghai Collaborative Innovation Center of Industrial Transformation of Hospital TCM Preparation, and the Outstanding PI Project of Guanghua Hospital, Changning District, Shanghai.

Data availability

All data related to this study can be obtained from the authors on reasonable request.

Declarations

Consent for publication

All the authors approved the final version of the manuscript.

Competing interests

The authors declare that they have no competing interests.

Received: 3 December 2023 Accepted: 19 May 2024

Published online: 08 July 2024

References

- Shams S, Martinez JM, Dawson JRD, Flores J, Gabriel M, Garcia G, Guevara A, Murray K, Pacifici N, Vargas MV, Voelker T, Hell JF, Ashouri JW. The Therapeutic Landscape of Rheumatoid Arthritis: Current State and Future Directions. 1663–9812 (Print).
- Bindu S, Mazumder S, Bandyopadhyay U. Non-steroidal anti-inflammatory drugs (NSAIDs) and organ damage: a current perspective. *Biochem Pharmacol.* 2020;180:114147.
- Chen M, Fu W, Xu H, Liu CJ. Pathogenic mechanisms of glucocorticoid-induced osteoporosis. *Cytokine Growth Factor Rev.* 2023;70:54–66.
- Costello RE, Yimer BB, Roads P, Jani M, Dixon WG. Glucocorticoid use is associated with an increased risk of hypertension. *Rheumatology (Oxford).* 2021;60(1):132–9.
- Jensen C, Teng Y. Is It Time to Start Transitioning From 2D to 3D Cell Culture?. 2296–889X (Print).
- Breslin S, O'Driscoll L. Three-dimensional cell culture: the missing link in drug discovery. *Drug Discov Today.* 2013;18(5–6):240–9.
- Alhaque S, Themis M, Rashidi H. Three-dimensional cell culture: from evolution to revolution. *Philos Trans R Soc Lond B Biol Sci.* 2018;373:1750.
- Pickl M, Ries CH. Comparison of 3D and 2D tumor models reveals enhanced HER2 activation in 3D associated with an increased response to trastuzumab. *Oncogene.* 2009;28(3):461–8.
- Herreros-Pomares A, Zhou X, Calabuig-Fariñas S, Lee S-J, Torres S, Esworthy T, Hann SY, Jantus-Lewintre E, Camps C, Zhang LG. 3D printing novel in vitro cancer cell culture model systems for lung cancer stem cell study. *Mater Sci Eng, C.* 2021;122:111914.
- Čiužas D, Krugly E, Petrikaitė V. Fibrous 3D printed poly(ϵ)caprolactone tissue engineering scaffold for in vitro cell models. *Biochem Eng J.* 2022;185:108531.
- Jung SS, Son J, Yi SJ, Kim K, Park HS, Kang H-W, Kim HK. Development of Müller cell-based 3D biomimetic model using bioprinting technology. *Biomed Mater.* 2023;18(1):015009.
- Yang GH, Kim W, Kim J, Kim G. A skeleton muscle model using GelMA-based cell-aligned bioink processed with an electric-field assisted 3D/4D bioprinting. *Theranostics.* 2021;11(1):48–63.
- Huang J, Huang Z, Liang Y, Yuan W, Bian L, Duan L, Rong Z, Xiong J, Wang D, Xia J. 3D printed gelatin/hydroxyapatite scaffolds for stem cell chondrogenic differentiation and articular cartilage repair. *Biomater Sci.* 2021;9(7):2620–30.
- Gatenholm B, Lindahl C, Britberg M, Simonsson S. Collagen 2A type b induction after 3d bioprinting chondrocytes in situ into osteoarthritic chondral tibial lesion. *Cartilage.* 2021;13(2_suppl):1755s–69s.
- Hu G, Liang Z, Fan Z, Yu M, Pan Q, Nan Y, Zhang W, Wang L, Wang X, Hua Y, Zhou G, Ren W. Construction of 3D-Bioprinted cartilage-mimicking substitute based on photo-crosslinkable Wharton's jelly bioinks for full-thickness articular cartilage defect repair. *Materials Today Bio.* 2023;21:100695.
- Liu Y, Peng L, Li L, Huang C, Shi K, Meng X, Wang P, Wu M, Li L, Cao H, Wu K, Zeng Q, Pan H, Lu WW, Qin L, Ruan C, Wang X. 3D-bioprinted BMSC-laden biomimetic multiphasic scaffolds for efficient repair of osteochondral defects in an osteoarthritic rat model. *Biomaterials.* 2021;279:121216.
- Singh YP, Moses JC, Bandyopadhyay A, Mandal BB. 3D Bioprinted silk-based in vitro osteochondral model for osteoarthritis therapeutics. *Adv Healthc Mater.* 2022;11(24):e2200209.
- Gomes JM, Marques CF, Rodrigues LC, Silva TH, Silva SS, Reis RL. 3D bioactive ionic liquid-based architectures: an anti-inflammatory approach for early-stage osteoarthritis. *Acta Biomater.* 2024;173:298–313.
- Mei X, Tong J, Zhu W, Zhu Y. lncRNA-NR024118 overexpression reverses LPS-induced inflammatory injury and apoptosis via NF- κ B/Nrf2 signaling in ATDC5 chondrocytes. *Mol Med Rep.* 2019;20(4):3867–73.
- Ying H, Wang Y, Gao Z, Zhang Q. Long non-coding RNA activated by transforming growth factor beta alleviates lipopolysaccharide-induced inflammatory injury via regulating microRNA-223 in ATDC5 cells. *Int Immunopharmacol.* 2019;69:313–20.
- Jiang R, Hao P, Yu G, Liu C, Yu C, Huang Y, Wang Y. Kaempferol protects chondrogenic ATDC5 cells against inflammatory injury triggered by lipopolysaccharide through down-regulating miR-146a. *Int Immunopharmacol.* 2019;69:373–81.
- Wang XC, Zhao NJ, Guo C, Chen JT, Song JL, Gao L. Quercetin reversed lipopolysaccharide-induced inhibition of osteoblast differentiation through the mitogen-activated protein kinase pathway in MC3T3-E1 cells. *Mol Med Rep.* 2014;10(6):3320–6.
- Bourebaba L, Michalak I, Baouche M, Kucharczyk K, Fal AM, Marycz K. Cladophora glomerata enriched by biosorption with Mn(II) ions alleviates lipopolysaccharide-induced osteomyelitis-like model in MC3T3-E1, and 4B12 osteoclastogenesis. *J Cell Mol Med.* 2020;24(13):7282–300.
- Jin F, Liao L, Zhu Y. MiR-467b alleviates lipopolysaccharide-induced inflammation through targeting STAT1 in chondrogenic ATDC5 cells. *Int J Immunogenet.* 2021;48(5):435–42.
- Wang Y, Yu C, Zhang H. Lipopolysaccharides-mediated injury to chondrogenic ATDC5 cells can be relieved by Sinomenine via downregulating microRNA-192. *Phytother Res PTR.* 2019;33(7):1827–36.
- Li W, Zhang H, Chen J, Tan Y, Li A, Guo L. N-acetyl Cysteine inhibits cell proliferation and differentiation of Lps-induced MC3T3-E1 cells via regulating inflammatory cytokines. *Curr Pharm Biotechnol.* 2023;24(3):450–9.
- Yin W, Liu S, Dong M, Liu Q, Shi C, Bai H, Wang Q, Yang X, Niu W, Wang L. A new NLRP3 inflammasome inhibitor, dioscin, promotes osteogenesis. *Small.* 2020;16(1):e1905977.
- Guo C, Yuan L, Wang JG, Wang F, Yang XK, Zhang FH, Song JL, Ma XY, Cheng Q, Song GH. Lipopolysaccharide (LPS) induces the apoptosis and inhibits osteoblast differentiation through JNK pathway in MC3T3-E1 cells. *Inflammation.* 2014;37(2):621–31.
- Liu H, Hao W, Wang X, Su H. miR-23b targets Smad 3 and ameliorates the LPS-inhibited osteogenic differentiation in preosteoblast MC3T3-E1 cells. *J Toxicol Sci.* 2016;41(2):185–93.
- He S, Zhang H, Lu Y, Zhang Z, Zhang X, Zhou N, Hu Z. Nampt promotes osteogenic differentiation and lipopolysaccharide-induced interleukin-6 secretion in osteoblastic MC3T3-E1 cells. *Aging.* 2021;13(4):5150–63.
- Chen X, Wen J, Liu C, Guo D. KLF4 downregulates FGF21 to activate inflammatory injury and oxidative stress of LPS-induced ATDC5 cells via SIRT1/NF- κ B/p53 signaling. *Mol Med Rep.* 2022;25:5.
- Chen W, Zheng H, Zhang X, Xu Y, Fu Z, Ji X, Wei C, An G, Tan M, Zhou M. Columbianetin alleviates lipopolysaccharides (LPS)-induced inflammation and apoptosis in chondrocyte through activation of autophagy by inhibiting serum and glucocorticoid-induced protein kinase 1 (SGK1) expression. *Bioengineered.* 2022;13(2):4051–62.
- Guo C, Wang S-L, Xu S-T, Wang J-G, Song G-H. SP600125 reduces lipopolysaccharide-induced apoptosis and restores the early-stage differentiation of osteoblasts inhibited by LPS through the MAPK pathway in MC3T3-E1 cells. *Int J Mol Med.* 2015;35(5):1427–34.

34. Chen S, Wang Q, Wu C, Zhao X, Xu H, Shi Q, Liang Q. Efficacy and mechanism of action of Danggui Niantong decoction against acute gouty arthritis in a mouse model: an experimental study. *Chinese General Practice*. 2021;24(24):3116–21+3128.
35. Yao L, Wang S. Effect of Danggui Niantong Decoction on joint swelling and tissue inflammatory factors for rats with acute gouty arthritis. *J Sichuan Tradit Chin Med*. 2018;36(12):37–9.
36. Zeng W, Yan Y, Zhang F, Zhang C, Liang W. Chrysin promotes osteogenic differentiation via ERK/MAPK activation. *Protein Cell*. 2013;4(7):539–47.
37. Hou Z, Wang Z, Tao Y, Bai J, Yu B, Shen J, Sun H, Xiao L, Xu Y, Zhou J, Wang Z, Geng D. KLF2 regulates osteoblast differentiation by targeting of Runx2. *Lab Invest*. 2019;99(2):271–80.
38. Jadlowiec J, Koch H, Zhang X, Campbell PG, Seyedain M, Sfeir C. Phosphoryn regulates the gene expression and differentiation of NIH3T3, MC3T3-E1, and human mesenchymal stem cells via the integrin/MAPK signaling pathway. *J Biol Chem*. 2004;279(51):53323–30.
39. Duval K, Grover H, Han LH, Mou Y, Pegoraro AF, Fredberg J, Chen Z. Modeling physiological events in 2D vs. 3D cell culture. *Physiology (Bethesda)*. 2017;32(4):266–77.
40. Owida HA, Kuiper NL, Yang Y. Maintenance and acceleration of pericellular matrix formation within 3D cartilage cell culture models. *Cartilage*. 2021;13(2_suppl):847s–61s.
41. Tevlek A, Aydin HM. Multi-layered in vitro 3D-bone model via combination of osteogenic cell sheets with electrospun membrane interlayer. *J Biomater Appl*. 2021;36(5):818–33.
42. Esmaeili A, Hosseini S, Kamali A, Hosseinzadeh M, Shekari F, Baghaban Eslaminejad M. Co-aggregation of MSC/chondrocyte in a dynamic 3D culture elevates the therapeutic effect of secreted extracellular vesicles on osteoarthritis in a rat model. *Sci Rep*. 2022;12(1):19827.
43. Wolff A, Frank M, Staehle S, Peters K. A comparative study on the adipogenic differentiation of mesenchymal stem/stromal cells in 2D and 3D culture. *Cells*. 2022;11:8.
44. Sung T-C, Heish C-W, Lee HH-C, Hsu J-Y, Wang C-K, Wang J-H, Zhu Y-R, Jen S-H, Hsu S-T, Hirad AH, Alarfaj AA, Higuchi A. 3D culturing of human adipose-derived stem cells enhances their pluripotency and differentiation abilities. *J Mater Sci Technol*. 2021;63:9–17.
45. Fang Y, Eglén RM. Three-dimensional cell cultures in drug discovery and development. *SLAS Discov*. 2017;22(5):456–72.
46. Biju TS, Priya VV, Francis AP. Role of three-dimensional cell culture in therapeutics and diagnostics: an updated review. *Drug Deliv Transl Res*. 2023;13(9):2239–53.
47. Peck Y, Leom LT, Low PFP, Wang DA. Establishment of an in vitro three-dimensional model for cartilage damage in rheumatoid arthritis. *J Tissue Eng Regen Med*. 2018;12(1):e237–49.
48. Rosser J, Bachmann B, Jordan C, Ribitsch I, Haltmayer E, Gueltekin S, Junttila S, Galik B, Gyenesei A, Haddadi B, Harasek M, Egerbacher M, Ertl P, Jenner F. Microfluidic nutrient gradient-based three-dimensional chondrocyte culture-on-a-chip as an in vitro equine arthritis model. *Mater Today Bio*. 2019;4: 100023.
49. Samavedi S, Diaz-Rodriguez P, Erndt-Marino JD, Hahn MS. A three-dimensional Chondrocyte-Macrophage coculture system to probe inflammation in experimental osteoarthritis. *Tissue Eng Part A*. 2017;23(3–4):101–14.
50. Li H, Davison N, Moroni L, Feng F, Crist J, Salter E, Bingham CO, Elisseeff J. Evaluating osteoarthritic chondrocytes through a novel 3-dimensional in vitro system for cartilage tissue engineering and regeneration. *Cartilage*. 2012;3(2):128–40.
51. Lin J, Sun A.R, Li J, Yuan T, Cheng W, Ke L, Chen J, Sun W, Mi S, Zhang P. A three-dimensional co-culture model for rheumatoid arthritis pannus tissue. 2296–4185 (**Print**).
52. Philippon EML, van Rooijen LJE, Khodadust F, van Hamburg JP, van der Laken CJ, Tas SW. A novel 3D spheroid model of rheumatoid arthritis synovial tissue incorporating fibroblasts, endothelial cells, and macrophages. *Front Immunol*. 2023;14:1188835.
53. Liu G, Wang Y, Zhang M, Zhang Q. Long non-coding RNA THRIL promotes LPS-induced inflammatory injury by down-regulating microRNA-125b in ATDC5 cells. *Int Immunopharmacol*. 2019;66:354–61.
54. Sui C, Zhang L, Hu Y. MicroRNA-let-7a inhibition inhibits LPS-induced inflammatory injury of chondrocytes by targeting IL6R. *Mol Med Rep*. 2019;20(3):2633–40.
55. Fan L, Li M, Cao FY, Zeng ZW, Li XB, Ma C, Ru JT, Wu XJ. Astragalus polysaccharide ameliorates lipopolysaccharide-induced cell injury in ATDC5 cells via miR-92a/KLF4 mediation. *Biomed Pharmacother*. 2019;118: 109180.
56. Luan L, Liang Z. Tanshinone IIA protects murine chondrogenic ATDC5 cells from lipopolysaccharide-induced inflammatory injury by down-regulating microRNA-203a. *Biomed Pharmacother*. 2018;103:628–36.

Publisher's Note

Springer Nature remains neutral with regard to jurisdictional claims in published maps and institutional affiliations.